3

Propagation Models for the Characterization of the Indoor UWB Channel

Francisco Saez de Adana
Universidad de Alcala
Spain

1. Introduction

Ultra-wideband (UWB) technology has developed rapidly over the past several years. This technology is especially attractive in high-data-rate and short-range wireless communications. These applications make UWB technology suitable for indoor mobile communication applications, such as wireless personal-area networks (WPAN). This interest has motivated the study of the propagation of the UWB signals in indoor environments as an important task for the implementation of WPANs.

In the last decades, significant effort has been focused on the characterization of the indoor channel for narrowband systems. Statistical (Motley & Keenan, 1990; Saleh & Valenzuela, 1987; Seidel & Rappaport, 1992; Tornevik et al., 1993) and deterministic (Lauer et al., 1984; Saez de Adana et al., 2000; Tarng et al., 1997; Whitman et al., 1995) models have been used most frequently in these studies. The statistical models are based on the obtention of closed formulas to characterize the propagation channel. These formulas are derived from the data obtained from measurement campaigns in different environments. Alternatively, the deterministic models are based mostly on the use of ray-tracing techniques (Saez de Adana et al., 2000; Tarng et al., 1997; Whitman et al., 1995) to predict the multipath phenomena and the Uniform Theory of Diffraction (UTD) technique (Kouyoumjian & Pathak, 1974) to calculate the received power or the propagation losses. However, the features of the UWB systems (with bandwidth in the range of GHz) render the conventional narrowband propagation models, both statistical and deterministic, inapplicable. These models are based primarily on frequency-domain analysis, while UWB requires a time-domain analysis due to its wide bandwidth. Therefore, special models must be used to predict the signal propagation in UWB systems. Although the number of statistical models developed for UWB systems is not as extensive as that for narrowband systems, some recent examples can be found in the literature (Cassioli et al., 2001, 2002, Dabin et al., 2006; Molisch et al., 2006). These models have been obtained, as in the case of narrowband systems, by obtaining closed expressions that fit the behavior of the received signal measured in several locations in a measurement campaign.

Regarding the deterministic models, frequency-domain UTD can be applied, performing an analysis at several frequencies and obtaining the time response using an Inverse Fourier Transform. However, this procedure is computationally inefficient in comparison to direct analysis in the time domain. Instead, the Time-Domain Uniform Theory of Diffraction (TD-UTD) was developed to obtain a solution in the time domain for the reflection and the

diffraction of a transient electromagnetic wave. The inclusion of the multipath phenomena in this theory and the analysis in the TD makes this technique suitable for UWB applications. TD-UTD was first developed by Veruttipong and Kouyoumjian (Veruttipong & Kouyoumjian, 1979), who applied the inverse Laplace transform to the frequency-domain UTD formulation. Later, Rousseau and Pathak (Rousseau & Pathak, 1995) presented closed-form solutions for the diffraction by an edge by modifying the formulation presented in (Veruttipong & Kouyoumjian, 1979). The results obtained in (Rousseau & Pathak, 1995) can be directly applied to develop a method for the calculation of the indoor propagation in UWB systems.

In this chapter, the formulation of both a statistical approach and a deterministic approach are presented. The statistical approach has been selected from the available literature because it seems very suitable for the case of UWB systems. The deterministic formulation was developed by the author of this chapter and consists of modifying the formulation presented in (Rousseau & Pathak, 1995) to introduce the contribution of lossy materials present in the indoor environment to reflection, transmission and diffraction. The goal is to obtain the reflection, transmission or diffraction coefficients using an Analytical Time Transform (ATT) from their expressions in the frequency domain. In addition, multiple interactions are also considered in this approach. These interactions include multiple reflections and transmissions and the interactions between reflected and diffracted rays. Thus, both reflection-diffraction and diffraction-reflection interactions are included. These interactions, which are obtained in the frequency domain from the product of the coefficients involved in the propagation mechanisms, can also be computed in the time domain by convolving those coefficients instead.

The deterministic approach is completed, including the analysis of a real site, which proves the validity of the model and its ability to analyze realistic environments. Some experimental measurements and comparisons with the predictions of the proposed model are presented in this chapter.

2. Statistical approach

The statistical models are obtained based on the statistical analysis of the experimental data. Some measurements are performed for a given scenario and a propagation model is obtained based on these results after the statistical analysis. In this chapter, one of these statistical models is presented. This model was obtained from measurements performed in a typical modern office building (Cassioli et al., 2002).

This propagation model provides all the parameters and distributions necessaries to obtain the power delay profile. First, the attenuation of the received power satisfies the following expression, dependent on the distance:

$$L(\mathrm{dB}) = \begin{cases} 20.4\log\left(\dfrac{d}{d_0}\right) & d \le 11\ \mathrm{m} \\ -56 + 74\log\left(\dfrac{d}{d_0}\right) & d > 11\ \mathrm{m} \end{cases} \quad (1)$$

The small-scale average-power delay profile (SSA-PDP) accomplishes the following expression:

$$g(\tau) = \sum_{k=1}^{N_{bins}} G_k \delta(\tau - \tau_k) \tag{2}$$

where $g(\tau)$ is the average energy received with delay τ, normalized to the total energy at one meter, and N_{bins} is the number of bins selected in the observation window. The idea of quantizing the delay axis into bins comes from (Rappaport et al., 1991). In that way, the local PDP is obtained by integrating the received power within each bin. This local PDP is expressed in terms of the pairs $\{G_k, \tau_k\}$, where G_k is the ratio between the energy received at a distance d and the total energy received at one meter. This value is called the energy gain and is obtained over a bin with size $\Delta\tau$ beginning with a delay $\tau_k = (k-1)\Delta\tau$. In the model proposed in (Cassioli et al., 2002), $\Delta\tau$ =2 ns.
An exponential decay from the second bin can be assumed. Therefore,

$$g(\tau) = G_1 \delta(\tau - \tau_1) + \sum_{k=2}^{N_{bins}} G_2 \delta(\tau - \tau_k) e^{\frac{-(\tau_k - \tau_2)}{\varepsilon}} \tag{3}$$

where ε is the decay constant of the SSA-PDP.
The total average energy received in the observation interval T is

$$G_{tot} = \int_0^T g(\tau) d\tau = G_1 + \sum_{k=2}^{N_{bins}} G_2 e^{\frac{-(\tau_k - \tau_2)}{\varepsilon}} \tag{4}$$

Because the second term of expression (4) is a geometric series,

$$G_{tot} = G_1 \left[1 + rF(\varepsilon)\right] \tag{5}$$

where $r = \frac{G_2}{G_1}$ is the power ratio and

$$F(\varepsilon) = \frac{1 - e^{\frac{-(N_{bins}-1)\Delta\tau}{\varepsilon}}}{1 - e^{\frac{-\Delta\tau}{\varepsilon}}} \tag{6}$$

A lognormal distribution around the mean value of the path loss can be considered:

$$G_{tot} = LN(-L; 4.3) \tag{7}$$

The average energy gains are obtained by inverting (5)

$$G_k = \begin{cases} \dfrac{G_{tot}}{1 + rF(\varepsilon)} & \text{for } k = 1 \\ \dfrac{G_{tot}}{1 + rF(\varepsilon)} r e^{\frac{-(\tau_k - \tau_2)}{\varepsilon}} & \text{for } k = 2, \ldots, N_{bins} \end{cases} \tag{8}$$

and therefore

$$g(\tau) = \frac{G_{tot}}{1 + rF(\varepsilon)} \left\{ \delta(\tau - \tau_1) + \sum_{k=2}^{N_{bins}} \left[r e^{\frac{-(\tau_k - \tau_2)}{\varepsilon}} \right] \delta(\tau - \tau_k) \right\} \tag{9}$$

This model characterizes the local PDP by the pairs $\{G_k, \tau_k\}$, as mentioned above, with $\tau_k = (k-1)\Delta\tau$ and G_k generated by a superposition of large- and small-scale statistics.
The first step is to obtain G_{tot} from (12). Next, the power ratio r and the decay factor ε are generated. These two values are treated as stochastic variables, modeled as lognormal variables according to the experience for narrowband systems shown in (Hashemi, 1979). The shape of the distribution is obtained from the measured data. Therefore,

$$\varepsilon = \mathrm{LN}(16.1;1.27) \tag{10}$$

$$\varepsilon = \mathrm{LN}(16.1;1.27) \tag{11}$$

and the width of the observation window is T=5.
With these parameters, SSA-PDP is completely specified by (9) and the local PDP can be obtained by obtaining the normalized energy gains $G_k^{(i)}$ of every bin k and every location i. $G_k^{(i)}$ are considered to be gamma-distributed independent variables with an average given by (8) and values m_k generated as independent truncated Gaussian variables

$$m_k = \mathrm{TN}(\mu_m(\tau_k); \sigma_m^2(\tau_k)) \tag{12}$$

with

$$\mu_m(\tau_k) = 3.5 - \frac{\tau_k}{73} \tag{13}$$

$$\sigma_m^2(\tau_k) = 1.84 - \frac{\tau_k}{160} \tag{14}$$

3. Deterministic approach

The classical UTD in the frequency domain obtains the field at an observation point inside an indoor environment as the sum of the contribution of different rays. These rays that started from the source reached that observation point either directly or after one or several reflections, diffractions, transmissions or combinations of these effects. Accordingly, the TD-UTD analytical impulse response in that environment can be obtained from an ATT, which consists of a one-sided Inverse Fourier Transform (IFT) of the frequency response, as can be seen in (Rousseau & Pathak, 1995; Veruttipong & Kouyoumjian, 1979), and can be written as

$$\overset{+}{f}_I(t) = \overset{+}{f}_I^{i}(t) + \overset{+}{f}_I^{r}(t) + \overset{+}{f}_I^{t}(t) + \overset{+}{f}_I^{d}(t) + \overset{+}{f}_I^{mr}(t) + \overset{+}{f}_I^{mt}(t) + \overset{+}{f}_I^{rd}(t) + \overset{+}{f}_I^{dr}(t) \tag{15}$$

where $\overset{+}{f}_I^{i}(t)$, $\overset{+}{f}_I^{r}(t)$, $\overset{+}{f}_I^{t}(t)$, $\overset{+}{f}_I^{d}(t)$, $\overset{+}{f}_I^{mr}(t)$, $\overset{+}{f}_I^{mt}(t)$, $\overset{+}{f}_I^{rd}(t)$ and $\overset{+}{f}_I^{dr}(t)$ are the analytical signal representations for the direct field $\overset{+}{f}_I^{i}(t)$, reflected field $\overset{+}{f}_I^{r}(t)$, transmitted field $\overset{+}{f}_I^{t}(t)$, diffracted field $\overset{+}{f}_I^{d}(t)$, multiply reflected field $\overset{+}{f}_I^{mr}(t)$, multiply transmitted $\overset{+}{f}_I^{mt}(t)$, reflected-diffracted-field $\overset{+}{f}_I^{rd}(t)$ and diffracted-reflected field $\overset{+}{f}_I^{dr}(t)$, respectively. Therefore, the impulse response shown in equation (15) includes all multipath phenomena, as mentioned previously. Each term in equation (15) will be described in the following sections.

3.1 Direct field

The contribution of the direct field to the impulse response is obtained as the ATT of the usual Geometrical Optics (GO) incident field and can be expressed by the following equation (Rousseau & Pathak, 1995):

$$\overset{+}{f}{}_I^i(t) = E_0^i \left| A_i(s_i) \right| \overset{+}{\delta}(t - s_i / c) \tag{16}$$

where E_0^i is the initial field value, which is constant with time and frequency, $A_i(s_i)$ is the spreading (or spatial divergence) factor for the direct ray, and s_i is the distance between the source and the observation point. The spreading factor for the direct ray is given by (Rousseau & Pathak, 1995):

$$A_i(s_i) = \sqrt{\frac{\rho_1^i \rho_2^i}{(\rho_1^i + s_i)(\rho_2^i + s_i)}} \tag{17}$$

where ρ_1^i and ρ_2^i are the principal radii of curvature of the incident wavefront at the observation point (see Figure 1).

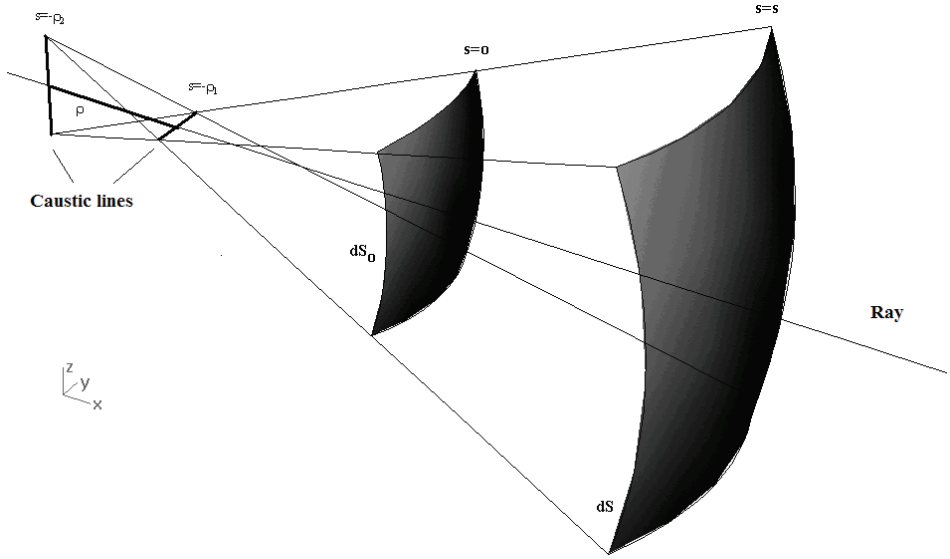

Fig. 1. Incident-ray wavefront

3.2 Reflected field

Similar to the case of the direct field, the contribution of the reflected field to the impulse response is obtained from the ATT of the classical GO expression in the frequency domain by the following equation:

$$\overset{+}{f}{}_I^r(t) = E_0^i \overset{\pm}{R}(t - s_i / c - s_r / c) \left| A_i(s_i) A_r(s_r) \right| \tag{18}$$

where s_i is, in this case, the distance between the source and the reflection point and s_r is the distance between the reflection point and the observation point. $A_r(s_r)$ is the spreading (or spatial divergence) factor for the reflected ray, which is expressed as (Rousseau & Pathak, 1995)

$$A_r(s_r) = \sqrt{\frac{\rho_1^r \rho_2^r}{(\rho_1^r + s_r)(\rho_2^r + s_r)}} \tag{19}$$

where ρ_1^r and ρ_2^r are the principal radii of curvature of the reflected wavefront at the observation point.

In equation (18), $\overline{\overline{R}}(t)$ is the TD dyadic reflection coefficient, which must be expressed in terms of its vertical and parallel components. These coefficients are obtained as the ATT of the classical Fresnel reflection coefficients (Yao et al., 2003) for a reflected surface composed of a lossy material. By performing this ATT, the parallel component can be expressed as

$$\overline{\overline{R}}_{||}(t) = K\overline{\overline{\delta}}(t) + \frac{4\kappa}{1-\kappa^2}\frac{e^{-at}}{t}\sum_{n=1}^{\infty}(-1)^{n+1} n K^n I_n(at) \tag{20}$$

where I_n is the modified Bessel function of order n and

$$K = \frac{1-\kappa}{1+\kappa} \qquad \kappa = \frac{\sqrt{\varepsilon_r - \cos^2\phi}}{\varepsilon_r \sin\phi} \qquad a = \frac{120\pi\sigma c}{2\varepsilon_r}$$

The perpendicular component is as follows:

$$\overline{\overline{R}}_{\perp}(t) = -\left[K\overline{\overline{\delta}}(t) + \frac{4\kappa}{1-\kappa^2}\frac{e^{-at}}{t}\sum_{n=1}^{\infty}(-1)^{n+1} n K^n I_n(at)\right] \tag{21}$$

where, in this case,

$$\kappa = \frac{\sin\phi}{\sqrt{\varepsilon_r - \cos^2\phi}} \qquad a = \frac{120\pi\sigma c}{2\varepsilon_r\left(1 - \frac{\cos^2\phi}{\varepsilon_r}\right)}$$

and the rest of parameters are the same.

3.3 Transmitted field

The impulse response for the transmitted field is analogous to that response for the reflected field and can be written as

$$\overline{\overline{f}}_I^r(t) = E_0^i \overline{\overline{T}}(t - s_i / c - s_t / c)\left|A_i(s_i)A_t(s_t)\right| \tag{22}$$

where s_i is, in this case, the distance between the source and the transmission point, s_t is the distance between the transmission point and the observation point, $A_t(s_t)$ is the spreading (or spatial divergence) factor for the transmitted ray, which can be obtained using expression (19) by replacing the radii of curvature of the reflected wavefront by those of the transmitted wavefront, and $\overline{\overline{T}}(t)$ is the TD dyadic transmission coefficient, which must also be expressed

in terms of its vertical and parallel components. The transmission coefficient can be obtained easily by considering that the relationship between the reflection and the transmission coefficients are the same in the time domain as in the frequency domain and is given by

$$\overset{+}{\underline{T}}(t) = I + \overset{+}{\underline{R}}(t) \tag{23}$$

where I is the identity matrix.

3.4 Diffracted field

In the case of diffraction, its contribution to the impulse response is given by the ATT of the UTD expression for the frequency domain as follows:

$$\overset{+}{f}{}_I^d(t) = E_0^i \overset{+}{\underline{D}}(t - s_i / c - s_d / c)\left|A_i(s_i)A_d(s_d)\right| \tag{24}$$

where s_i is, in this case, the distance between the source and the diffraction point, s_d is the distance between the diffraction point and the observation point, $A_d(s^d)$ is the spreading (or spatial divergence) factor for the reflected ray given by (Rousseau & Pathak, 1995)

$$A_d(s_d) = \sqrt{\frac{\rho^s}{(\rho^s + s_d)\cdot s_d}} \tag{25}$$

where ρ^s is the principal radius of curvature of the diffracted wavefront at the observation point.

On the other hand, $\overset{+}{\underline{D}}(t)$ is the TD dyadic diffraction coefficient, which must be expressed in terms of its components with respect to the edge-fixed system. The diffraction coefficients for a PEC wedge are obtained as the sum of four terms, as in (Rousseau & Pathak, 1995). If the lossy materials are included in the formulation, the last two terms corresponding to the contribution of the reflected shadow boundary must include the effect of the lossy reflection coefficient. In the frequency domain, this inclusion is performed by a product. Therefore, the convolution between the reflection coefficient and these two terms of the diffraction coefficient must instead be performed in the time domain. Performing this convolution results in the following expression for the diffraction coefficients:

$$\overset{+}{\underline{D}}_{\beta,\varphi}(t) = \overset{+}{D}_1(t) + \overset{+}{D}_2(t) + \overset{+}{\underline{R}}_{\perp,\parallel} * \left[\overset{+}{D}_3(t) + \overset{+}{D}_4(t)\right] \tag{26}$$

The expressions for $\overset{+}{D}_1(t)$, $\overset{+}{D}_2(t)$, $\overset{+}{D}_3(t)$ and $\overset{+}{D}_4(t)$ are given as follows (Rousseau & Pathak, 1995):

$$\overset{+}{D}_1(t) = A_0 \cot\left[\frac{\pi + (\phi - \phi')}{2n}\right] \overset{+}{F}\left[L^i a^+(\phi - \phi')\right] \tag{27}$$

$$\overset{+}{D}_2(t) = A_0 \cot\left[\frac{\pi - (\phi - \phi')}{2n}\right] \overset{+}{F}\left[L^i a^-(\phi - \phi')\right] \tag{28}$$

$$\overset{+}{D}_3(t) = A_0 \cot\left[\frac{\pi + (\phi + \phi')}{2n}\right] \overset{+}{F}\left[L^{rn} a^{+}(\phi + \phi')\right] \tag{29}$$

$$\overset{+}{D}_4(t) = A_0 \cot\left[\frac{\pi - (\phi + \phi')}{2n}\right] \overset{+}{F}\left[L^{ro} a^{-}(\phi + \phi')\right] \tag{30}$$

with $A_0 = \dfrac{-1}{2n\sqrt{2\pi}\sin\beta_0^i}$, where β_0^i is the angle between the direction of incidence and the vector of the edge and $\overset{+}{F}(x,t) = \dfrac{\sqrt{x/\pi}\left(j\sqrt{t} + \sqrt{x/c}\right)}{\sqrt{t}\left(t + x/c\right)}$.

The L^i are distance parameters associated with the incident shadow boundaries and are the same as in the frequency domain. These parameters are given by

$$L^i = \frac{s_d\,(\rho_e^i + s_d)\,\rho_1^i \rho_2^i}{\rho_e^i\,(\rho_1^i + s_d)\,(\rho_2^i + s_d)} \sin^2\beta_0^i \tag{31}$$

$$L^{ro,n} = \frac{s_d\,(\rho_e^{ro,n} + s_d)\,\rho_1^{ro,n} \rho_2^{ro,n}}{\rho_e^{ro,n}\,(\rho_1^{ro,n} + s_d)\,(\rho_2^{ro,n} + s_d)} \sin^2\beta_0^i \tag{32}$$

where ρ_1^i is the radius of curvature 1 of the incident wavefront at the edge, ρ_2^i is the radius of curvature 2 of the incident wavefront at the edge, ρ_e^i is the radius of curvature of the incident wavefront at edge-fixed plane of incidence, $\rho_1^{ro,rn}$ is the radius of curvature 1 of the reflected wavefront from the o and n faces, respectively, $\rho_2^{ro,rn}$ is the radius of curvature 2 of the reflected wavefront from the o and n faces, respectively, and $\rho_e^{ro,rn}$ is the radius of curvature of the reflected wavefront from the plane containing the reflected ray and the edge.

The function $a^{\pm}$ in the expressions (27)-(30) is given by

$$\begin{aligned} a^{\pm}(\beta^{\pm}) &= 2\cos^2\left(\frac{2n\pi N^{\pm} - \beta^{\pm}}{2}\right) \\ \beta^{\pm} &= \phi^d \pm \phi^i \\ 2\pi n N^{+} - (\phi^d \pm \phi^i) &= \pi \\ 2\pi n N^{-} - (\phi^d \pm \phi^i) &= -\pi \end{aligned} \tag{33}$$

The geometrical parameters involved in the calculation of the diffraction coefficients are the same as in the frequency domain as shown in Figure 2 and are explained in (Kouyoumjian & Pathak, 1974).

3.5 Multiple reflected and multiple transmitted fields

The expressions for the m-order reflections and transmissions are easily derived recursively from the first-order effects. For instance, the second-order reflection is a single reflection where the source is set as the first reflection point and the incident field is the simple reflected field. Using this recursion, an m-order reflection that reaches the observation point would contribute the following term to the impulse response:

$$\overset{+}{f}{}_I^{mr}(t) = E_0^i \overset{+}{\bar{R}}_M \left| A_t(s_t) \right| \tag{34}$$

where

$$s_t = s_i + \sum_{j=1}^{m} s_r^j$$

$$A_t(s_t) = A_i(s_i) \prod_{j=1}^{m} A_r(s_r^j)$$

$$\overset{+}{\bar{R}}_M = \overset{+}{\bar{R}}_1(t - s_i / c - s_r^1 / c) * ..... * \overset{+}{\bar{R}}_m(t - s_i / c - \sum_{i=1}^{m} s_r^j / c)$$

s_r^j is the distance between the jth the (j+1)th reflection points (or between the mth reflection point and the observation point in the case of the last reflection).

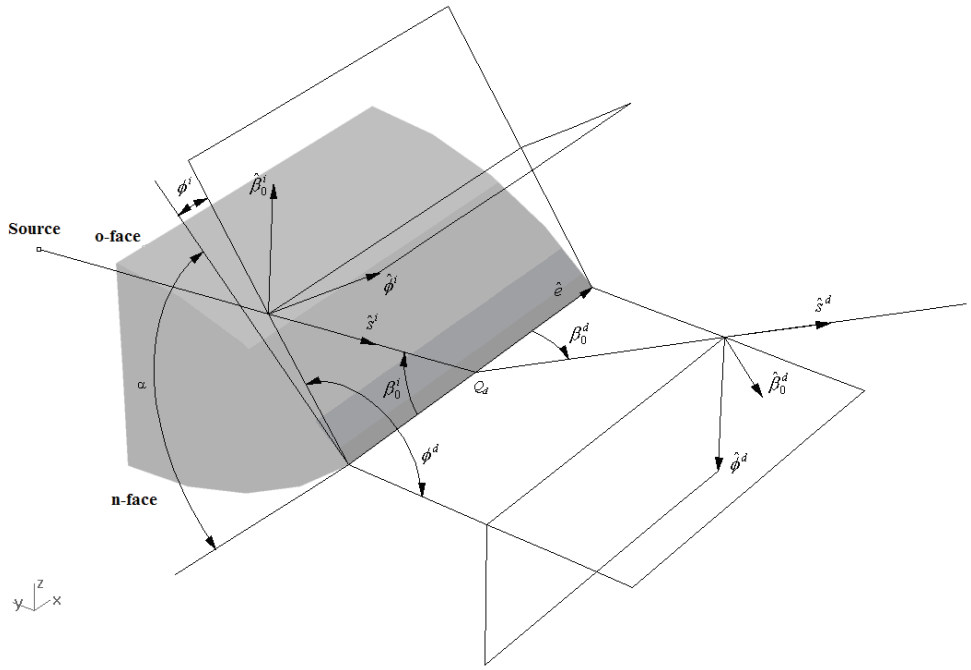

Fig. 2. Geometrical parameters and an edge-fixed system for the diffracted ray. In the figure, $\hat{e}$ is the vector of the edge, Q_d is the diffraction point, $\hat{s}^i$ and $\hat{s}^d$ are the incident and diffraction directions, respectively, β_0^i, β_0^d, ϕ^i and ϕ^d ($\beta_0^i = \beta_0^d = \beta_0$) are the diffraction angles, and $\hat{\beta}_0^i, \hat{\phi}^i$ and $\hat{\beta}_0^d, \hat{\phi}^d$ are the vectors of the edge-fixed system necessary to apply the diffraction coefficients. All parameters are explained in (Kouyoumjian & Pathak, 1974) because they are identical to those in the frequency domain case

Analogously, the m-order transmitted field is

$$f_I^{+mt}(t) = E_0^i \bar{\bar{T}}_M^{\pm} \left| A_t(s_t) \right| \tag{35}$$

where $\bar{\bar{T}}_M^{+}(t) = I + \bar{\bar{R}}_M^{+}(t)$.

3.6 Reflected-diffracted and diffracted-reflected fields

Following the same procedure as for multiple reflections, the contribution of the interaction between an edge and a reflecting surface to the impulse response can be written as

$$f_I^{+rd}(t) = E_0^i \left[\bar{\bar{R}}^{\pm}(t - s_i / c - s_r / c) * \bar{\bar{D}}^{\pm}(t - s_i / c - s_r / c - s_d / c) \right] \cdot \left| A_i(s_i) A_r(s_r) A_d(s_d) \right| \tag{36}$$

for the case of reflection-diffraction interactions and

$$f_I^{+dr}(t) = E_0^i \left[\bar{\bar{D}}^{\pm}(t - s_i / c - s_d / c) * \bar{\bar{R}}^{\pm}(t - s_i / c - s_r / c - s_d / c) \right] \cdot \left| A_i(s_i) A_d(s_d) A_r(s_r) \right| \tag{37}$$

for the case of diffraction-reflection interaction.
The meaning of these parameters is analogous to the previous effects.

3. Deterministic analysis of a realistic environment

The results of the deterministic approach presented in this chapter compared with measurements are shown in this section. The measurements were performed in a complex realistic site to investigate the validity of the approach. The measurements were done in the corridor of the second floor of the Polytechnic Building of the University of Alcala. Figure 3 shows the plan schematic of the measurement site. The dimensions of the scenario are 7.9x20.7 m. A 3D plane-facets model has been designed to represent the realistic environment composed of 77 facets. The material composition of the elements of the site was concrete for the walls, wood for the doors and glass for the windows. Table I lists the electrical properties of these three materials considered in our model.

Material	ε_r	**σ (S/m)**
Concrete	4.5	0.01
Wood	2	10^{-5}
Glass	6.5	10^{-12}

Table 1. Electrical characteristics of the materials for the measurement scenario

Several measurements were performed on the site. Examples of one Line-of-Sight (LOS) and one Non-Line-of-Sight (NLOS) case will be shown in this section. Figure 3 illustrates the position of the transmitter and the receiver in both cases. The coordinates of the transmitter were (1.60, 5.55, 1.10). The coordinates of the receivers were (5.0, 1.78, 1.10) for the LOS case and (9.55, 1.3, 1.10) for the NLOS case. All the coordinates are given in meters.
Measurements were conducted in the frequency domain using the network analyzer (VNA) Agilent E8362B. A linearly polarized double-ridged waveguide antenna was used as the

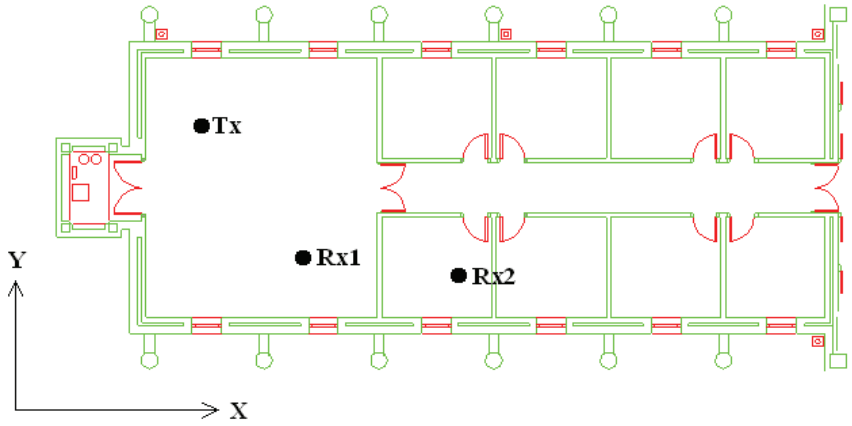

Fig. 3. Plan of the Polytechnic Building corridor of Alcala University and TX and RX placements for the measurement antennas

transmitter (TX) and as the receiver (RX). The frequency range of these antennas was 1 to 18 GHz. In this range, the average VSWR ratio was lower than 1.5.
Figure 4 shows an overview of the measurement setup. The VNA was set to transmit 3201 tones uniformly distributed over the 1-18 GHz frequency range. This transmission gave an excess delay of 188 ns and a maximum distance of 56.4 m. The temporal resolution for the 17 GHz frequency was 59 ps.

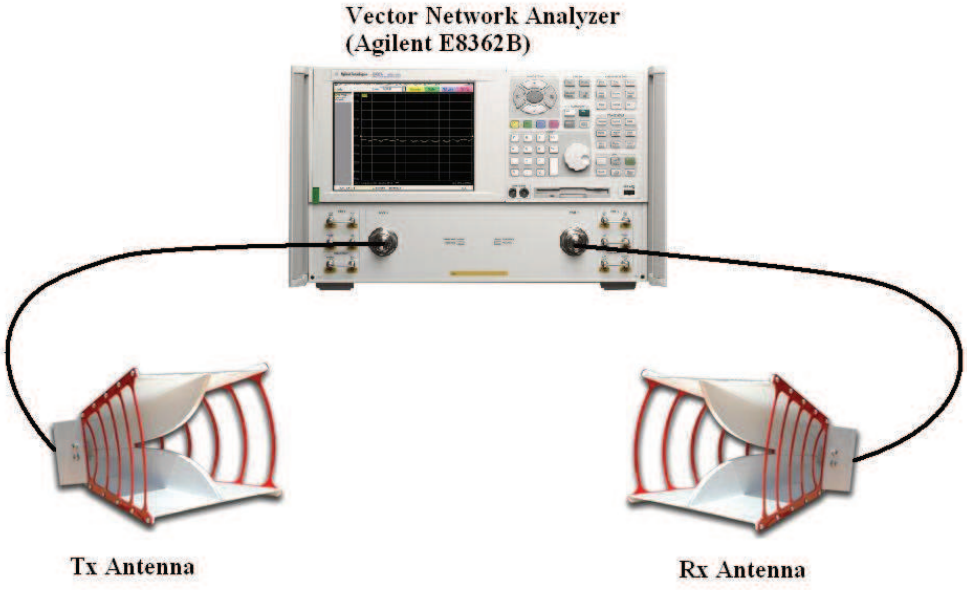

Fig. 4. Overview of the measurement setup

The input signal is expressed as a sum of a small number of simple expansion functions for a more efficient convolution with the TD-UTD impulse response. In this approach, the input signal is represented as the sum of waveforms with analytical signal representations that are simple poles in the complex time plane. This representation allows the convolution to be expressed in a closed form, thus speeding up computation. Moreover, the antenna transfer function is included in this representation. Equations (38) and (39) show the representation of the input signal and the closed form for the convolution, respectively.

$$\overset{+}{i}(t) = \frac{j}{\pi}\sum_{n=1}^{n}\frac{A_n}{t + j\tau_n} \tag{38}$$

$$\overset{+}{o}(t) = \frac{1}{2}\overset{+}{i}(t) * \overset{+}{f}(t) = \sum_{n=1}^{N} A_n \overset{+}{f}(t + j\tau_n) \tag{39}$$

The comparisons between the measurements and our approach for the normalized PDP in the LOS and the NLOS cases are shown in Figures 5 and 6, respectively. As can be seen, a good agreement between calculation and measurement is obtained in both cases. The mean errors were 3.5 dB for the LOS case and 4.6 dB for the NLOS case, which are very good for UWB applications.

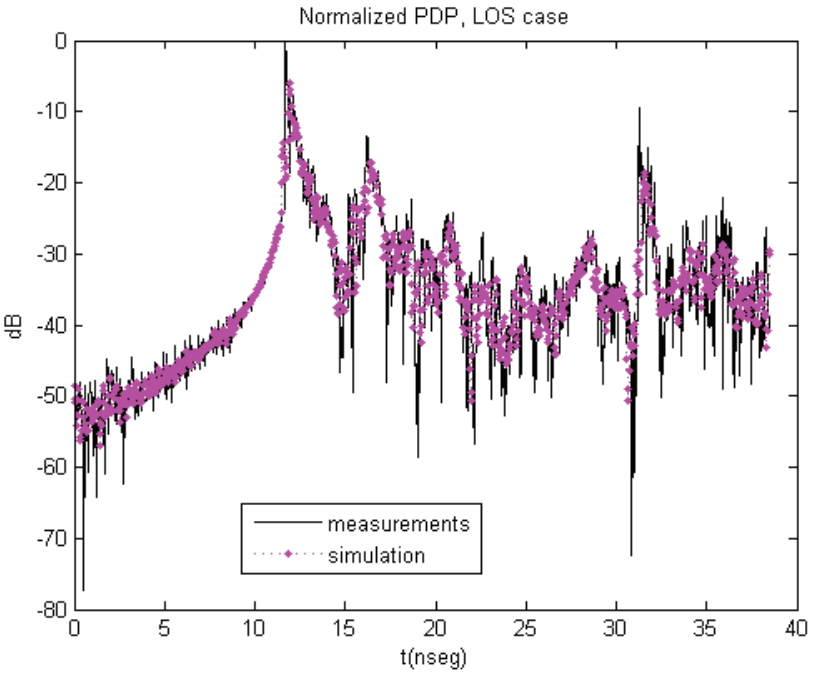

Fig. 5. Comparison between measurements and simulation for the LOS case

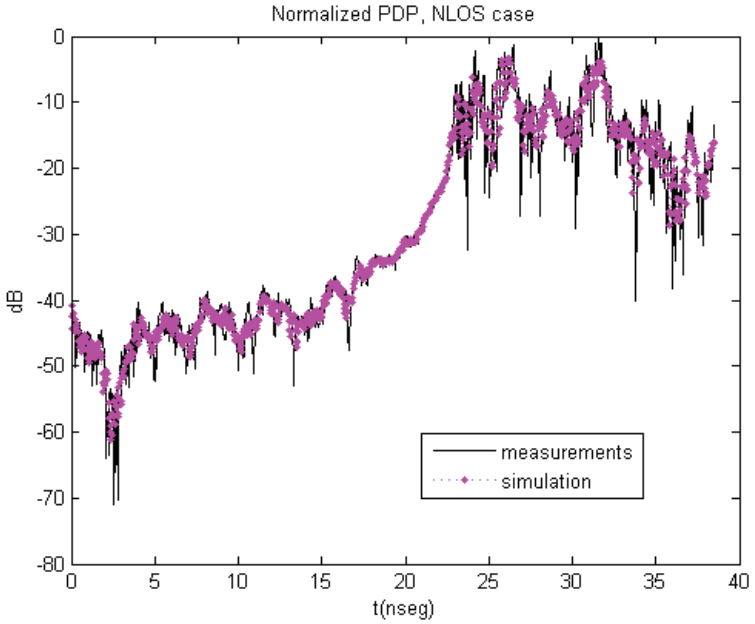

Fig. 6. Comparison between measurements and simulation for the NLOS case.

5. Acknowledgment

This work has been supported, in part, by the University of Alcalá, project UAH GC2010-004.

6. References

Cassioli, D.; Win, M. & Molisch, A. (2001). A Statistical Model for the UWB Indoor Channel, *Proceedings of 20015 53rd Vehicular Technology Conference,* pp. 1159, ISBN 0-7803-6728-6, Rhodes, Greece, May 6-9 2001.

Cassioli, D.; Win, M. & Molisch, A. (2002). The Ultra-Wide Band Indoor Channel: from Statistical Model to Simulations, *IEEE Journal on Selected Areas in Telecommunications,* Vol.20, No.6, (August 2002), pp. 1247-1257, ISSN 0733-8716.

Dabin, J.A.; Haimovich, A.M. & Grebel, H. (2006). A Statistical Ultra-Wide Band Indoor Channel Model and the Effects of Antenna Directivity on Path Loss and Multipath Propagation, *IEEE Journal on Selected Areas in Telecommunications* Vol.24, No.4, (April 2006), pp. 752-758, ISSN 0733-8716.

Hashemi, H. (1979). Simulation of the Urban Radio Propagation Channel. *IEEE Transactions on Vehicular Technology,* Vol. 28, No. 3 (March 1979), pp. 213-225, ISSN 0018-9545.

Kouyoumjian, R.G. & Pathak, P.H. (1974). A Uniform Geometrical Theory of Diffraction for an Edge in a Perfectly Conducting Surface, *Proceedings of the IEEE,* Vol.62, No.11 (November 1974), pp. 1448-1461, ISSN 0018-9219.

Lauer, A.; Bahr, A. & Wolff, I. (1984). FDTD Simulations of Indoor Propagation, *Proceedings of 1994 44th Vehicular Technology Conference,* pp. 883, ISBN 0-7803-1927-3, Stockholm, Sweden, June 8-10, 1994.

Molisch, A.; Cassioli, D.; Chong, C.; Emami, S.; Fort, A.; Kannan, B.; Karedal, J.; Kunisch, J.; Schantz, H.G.; Siwiak, K. & Win, M.Z. (2006). A Comprenhensive Standardized Model for Ultrawideband Propagation Channels, *IEEE Transactions on Antennas and Propagation,* Vol.54, No.11, (November 2006), pp. 3151-3166 ISSN 0018-926X.

Motley, A.J. & Keenan, J.M.P (1990). Radio Coverage in Buildings, *British Telecom Technological Journal, Special Issue Mobile Communications,* Vol.8, No. 1 (January 1990), pp. 19-24, ISSN 1358-3948.

Rappaport, T.S.; Siedel, S.Y. & Takamizawa, K. (1991). Statistical Channel Impulse Response Models for Factory and Open Plan Building Radio Communication System Design. *IEEE Transactions on Communications,* Vol.39, No.5, (May 1991), pp. 794-807, ISSN 0090-6778.

Rousseau, P.R. & Pathak, P.H. (1975). Time-Domain Uniform Theory of Diffraction for a Curved Wedge, *IEEE Transactions on Antennas and Propagation,* Vol.43, No.12, (December 1995), pp. 1375-1382, ISSN 0018-926X.

Saez de Adana, F.; Gutiérrez, O.; González, I.; Pérez, J. & Cátedra, M.F. (2000). Propagation Model Based on Ray-Tracing for the Design of Personal Communications, *IEEE Transactions on Vehicular Technology,* Vol.49, No.6, (November 2000), pp. 2105-2112, ISSN 0018-9545.

Saleh, A.A. & Valenzuela, R.A. (1987). A Statistical Model for Indoor Multipath Propagation, *IEEE Journal on Selected Areas on Communication,* Vol.5, No.2, (February 1987), pp. 128-137, ISSN 0733-8716.

Seidel, S.Y. & Rappaport, T.S. (1992). 914 MHz Path Loss Prediction Models for Indoor Wireless Communications in Multifloored Buildings, *IEEE Transactions on Antennas and Propagation,* Vol.40, No.2, (February 1992), pp. 207-217, ISSN 0018-926X.

Tarng, J.H.; Chang, W.R. & Hsu, B.J. (1997). Three-Dimensional Modelling of 900 MHz and 2.44 GHz Radio Propagation in Corridors, *IEEE Transactions on Vehicular Technology,* Vol.46, No.2, (May 1997), pp. 519-526 ISSN 0018-9545.

Tornevik, C.; Berg, J.E., Lotse, F. & Madfors, M. (1993). Propagation Models, Cell Planning and Channel Allocation for Indoor Applications of Cellular Systems, *Proceedings of 1993 43rd Vehicular Technology Conference,* pp. 867-870, ISBN 0-7803-1267-8, Secaucus, New Jersey, USA, May 18-20 1993.

Veruttipong, T. & Kouyoumjian, R.G. (1979). Early-Time Responses of Currents and Charges on Wedges and Strips, *Proceedings of the 1979 Antennas and Propagation Society International Symposium*, pp. 590-593, Seattle, Washington, USA, June 18-22 1979.

Whitman, G.M.; Kim, K.S. & Niver, E. (1995). A Theoretical Model for Radio Signal Attenuation inside Buildings, *IEEE Transactions on Vehicular Technology,* Vol.44, No.3, (August 1995), pp. 621-629, ISSN 0018-9545.

Yao, R.; Chen, Z. & Zhu, W. (2003). An Efficient Time-Domain Ray Model for UWB Indoor Multipath Propagation Channel, *Proceedings of 2003 58th Vehicular Technology Conference,* pp. 1293, ISBN 0-7803-7954-3, Orlando, Florida, USA, October 6-9, 2003.

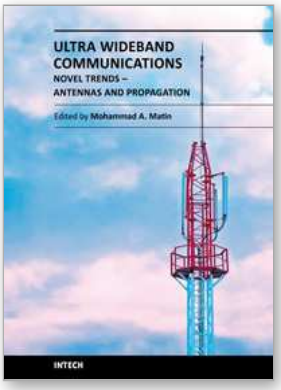

Ultra Wideband Communications: Novel Trends - Antennas and Propagation

Edited by Dr. Mohammad Matin

ISBN 978-953-307-452-8
Hard cover, 384 pages
Publisher InTech
Published online 09, August, 2011
Published in print edition August, 2011

This book explores both the state-of-the-art and the latest achievements in UWB antennas and propagation. It has taken a theoretical and experimental approach to some extent, which is more useful to the reader. The book highlights the unique design issues which put the reader in good pace to be able to understand more advanced research.

How to reference

In order to correctly reference this scholarly work, feel free to copy and paste the following:

Francisco Saez de Adana (2011). Propagation Models for the Characterization of the Indoor UWB Channel, Ultra Wideband Communications: Novel Trends - Antennas and Propagation, Dr. Mohammad Matin (Ed.), ISBN: 978-953-307-452-8, InTech, Available from: http://www.intechopen.com/books/ultra-wideband-communications-novel-trends-antennas-and-propagation/propagation-models-for-the-characterization-of-the-indoor-uwb-channel

INTECH
open science | open minds

InTech Europe
University Campus STeP Ri
Slavka Krautzeka 83/A
51000 Rijeka, Croatia
Phone: +385 (51) 770 447
Fax: +385 (51) 686 166
www.intechopen.com

InTech China
Unit 405, Office Block, Hotel Equatorial Shanghai
No.65, Yan An Road (West), Shanghai, 200040, China
中国上海市延安西路65号上海国际贵都大饭店办公楼405单元
Phone: +86-21-62489820
Fax: +86-21-62489821